Advances in Geo-Energy Research

Adv. Geo-Energy Res. Vol. 1, No. 1, p. 39-53, 2017
Ausasia Science and Technology Press

Invited review

Review on gas flow and recovery in unconventional porous rocks

Duanlin Lin[1], Jinjie Wang[2]*, Bin Yuan[3], Yinghao Shen[4]

[1]*Institute of Geophysics and Geomatics, China University of Geosciences, Wuhan 430074, P. R. China*

[2]*Faculty of Earth Resources, China University of Geosciences, Wuhan 430074, P. R. China*

[3]*Mewbourne School of Petroleum and Geological Engineering, University of Oklahoma, Norman, OK 73019, USA*

[4]*Bob L. Herd Department of Petroleum Engineering, Texas Tech University, Lubbock, TX 79409, USA*

(Received April 20, 2017; revised May 15, 2017; accepted May 18, 2017; published June 25, 2017)

Abstract: This study summarizes gas flow process in unconventional porous rocks, including the transportation in tight or shale reservoirs and the spontaneous imbibition happened in them. Fluids flow is greatly affected by the pore structure together with the pore size distribution of porous media. The MRI and BET measurement show peaks in pore throat radius ranging from 2 to 20 nm, whereas the diameter for methane and helium are 0.38 and 0.26 nm, respectively. Yet for different types of reservoir, distinct mechanisms should be utilized based on the flow regimes. Besides, experimental measurement techniques for conventional reservoirs are no long accurate enough for most of the unconventional reservoirs. New attempts have been implemented to obtain more valuable data for accurate reservoir prediction. By reviewing large numbers of articles, a clear and comprehensive map on the gas flow and recovery in unconventional reservoirs is made. Factors influencing the gas flow and recovery are investigated in detail for mathematical simulation process. Reservoir conditions and the sweep efficiency play an important role during gas production process. Besides, adsorbed gas contributes a lot to the total gas recovery. The overall investigations suggest that many parameters that influence the gas flow in unconventional porous rocks should be taken into consideration during the evaluation. Among them, permeability, adsorbed gas dynamics, stimulated reservoir volume as well as the unstimulated reservoir volume, and imbibition effect are the most important ones. This study provides valuable data and reasonable exploitations for characterizing gas flow and recovery in unconventional porous rocks.

Keywords: Unconventional rocks, gas flow, enhancing recovery, imbibition, fracture.

Citation: Lin, D., Wang, J., Yuan, B., et al. Review on gas flow and recovery in unconventional porous rocks. *Adv. Geo-Energy Res.* 2017, 1(1): 39-53, doi: 10.26804/ager.2017.01.04.

1. Introduction

Unconventional porous rocks refers to formations storing hydrocarbons, in which there exists ultra-low permeability matrix with nano/micro-pores, natural/artificial fractures, and some organic material (Javadpour et al., 2012; Loucks et al., 2012). The amount of unconventional hydrocarbons continues to grow as new reservoirs being discovered. For unconventional oil and gas reservoirs, it is well accepted that the production is from two sources: free gas in the pore and natural fracture space, and adsorbed gas on the pore surfaces of clay minerals and kerogen (Javadpour et al., 2007; Etminan et al., 2014). Due to the complex pore structure and multiscale pore sizes, they make the characterization of these reservoirs much more difficult and less accurate when the conventional techniques are applied.

Fluid flow in unconventional porous rocks play a significant role in forecasting the field production and draws more and more attention worldwide. Many academic articles have been published or cited by high-rank journals (Table 1). This number will continue to grow according to the data collected for the past 16 years, which is shown in Fig. 1.

Researchers are trying to make unconventional hydrocarbons economically and environmentally available. Gas flows through a pore network with ultra-low permeability, and the gas molecules will be of comparable size of nanopores under certain temperature and pressure conditions (Katsube, 2000; Javadpour et al., 2007; Javadpour, 2009; Curtis et al., 2010; Sondergeld et al., 2010). Javadpour et al. (2007) studied gas

*Corresponding authors. Email: wangjinjie06-2@163.com

Table 1. Top 10 journals for publishing the most articles and having the most citations related to the fluid flow in unconventional porous rocks and fractured reservoirs.

Ranking	Based on article number		Based on cited times		
	Journal	Number	Journal	year	Cited times
1	J. Pet. Sci. Eng.	204	Adv. Water Resour.	2002	424
2	J. Nat. Gas Sci. Eng.	193	Comput. Geosci.	2006	234
3	SPE Reserv. Eval. Eng.	155	J. Geol. Soc.	2007	211
4	SPE J.	123	Mar. Pet. Geol.	2000	201
5	Transp. Porous Media	89	J. Geophys. Res.	2000	169
6	Geothermics	82	Vadose Zone J.	2004	163
7	AAPG Bull.	71	Int. J. Coal Geol.	2012	162
8	J. Can. Pet. Technol.	65	J. Contam. Hydrol.	2003	161
9	Mar. Pet. Geol.	59	Mar. Pet. Geol.	2001	149
10	Energy Procedia	58	J. Geol. Soc.	2002	145

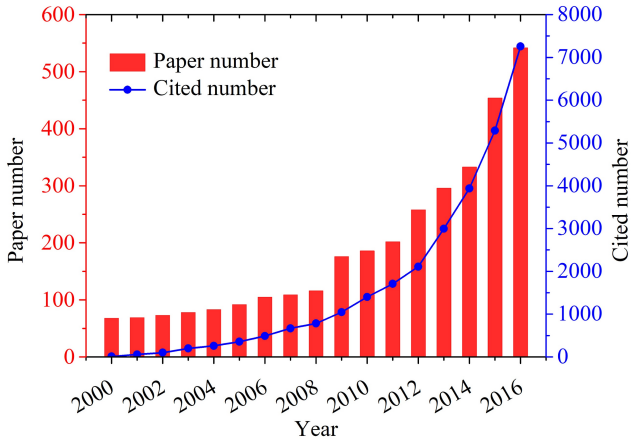

Fig. 1. The published papers about the topic of fluid flow in unconventional porous rocks and fractured reservoirs and their citations in the year from 2000 to 2016.

flow in nanoscale. Etminan et al. (2014) depicted the pressure history of the sample cell for each adsorption isotherm test. Qin et al. (2012) showed an apparatus for measuring the dynamic gas adsorption process by approximately retaining the pressure. A new Variable-volume Volumetric Method (VVM) has been designed by Wang et al. (2016a, 2016b) with the consideration of the dynamic gas adsorption/desorption process. With this technique, not only the amount of adsorbed gas stored in reservoir could be obtain, it also depicts the whole dynamic process of gas transport in unconventional rocks. As the reservoir bed and source rock, shale reservoirs are complex and anisotropic geologic systems, which makes it difficult but important to describe the dynamic process of shale gas production (Hill et al., 2007; Strapoc et al., 2010; Chen et al., 2011; Bustin and Bustin, 2012; Zhang et al., 2012; King Jr et al., 2015).

In this study, investigations are made on the characterization of fluids flow in unconventional porous rocks. Both theoretical study and experimental measurement will be shown here. First, permeability and gas transport in tight reservoirs are discussed. Some models are shown to understand the gas flow mechanism in nanopores for accurate numerical simulation of tight reservoirs. Second, gas transport dynamic is analyzed and the effect of adsorbed gas is explored on the gas production process. The dynamic gas production in shale is obtained according to the real time record of gas diffused out of and desorbed from shale. Third, we show some well-accepted interpretations of spontaneous imbibition as well as some advanced techniques for measuring this process.

2. Basic principles and models for gas transport in tight reservoirs

The gas shale is becoming more and more important with the development of gas reservoir exploitation and new techniques, i.e., hydraulic fracturing and horizontal drilling (Curtis et al., 2010). There are numbers of key challenges and difficulties faced by the industry, including environmental issues and commercial challenges (Rezaee, 2015). The fluids flow property in macropores is almost the same as in conventional gas reservoirs. The Darcy's Equation can be used to calculate the permeability and describe gas transports in this situation. In Darcy's Equation, the fluid-flow rate is linearly related to pressure gradient, which has been commonly used in numerical reservoir simulations and reservoir engineering analysis (Rezaee, 2015). However, in shale reservoirs, the gas transport is a complex and multiscale flow process, distinguished from that of the conventional gas reservoirs. It is essential to well understand the gas flow mechanism in nanopores for accurate numerical simulation of the shale gas reservoirs (Guo et al., 2015).

The permeability of shale gas reservoirs is extremely lower than that of the conventional gas reservoirs. When gas flows through a nano-scale pore network (ranging from a few to hundreds of nanometers), the gas molecules will be of comparable size of nanopores under certain temperature and pressure conditions (Katsube, 2000; Javadpour et al., 2007; Javadpour, 2009; Curtis et al., 2010; Sondergeld et al., 2010). The gas molecules may have stronger collisions with the pore

walls when the mean free path of gas molecules is larger than the size of pores. Thus, the concept of continuum flow may not be proper in such conditions (Javadpour et al., 2007). The mechanisms of gas transports in these pores are different from those in the conventional gas reservoirs.

The Knudsen number, K_n, is commonly used to identify flow regimes under different temperature and pressure conditions, which is the ratio of mean free path l to the pore diameter λ

$$K_n = \frac{l}{\lambda} \tag{1}$$

where l can be calculated as (Javadpour et al., 2007):

$$l = \frac{k_B T}{\sqrt{2}\pi\delta^2 p} \tag{2}$$

where k_B is the Boltzmann constant (1.3805×10^{-23} J/K), T is temperature; δ is the collision diameter of gas molecule and p is pressure.

Based on the Knudsen number, there usually have 4 flow regimes which are the free molecule flow ($K_n > 10$), the transition flow ($10^{-1} < K_n < 10$), the slip flow ($10^{-3} < K_n < 10^{-1}$) and the continuum flow ($K_n < 10^{-3}$) (as shown in Fig. 2). The rarefaction effects would become more pronounced when the Knudsen number gradually increases. Eventually, the continuum assumption will break down (Roy et al., 2003). It is important to find an equation or a method to describe the flow beyond the limit of slip flow when K_n is over 0.1. Some basic models of gas transport in tight reservoirs have been proposed to study different factors of flow mechanisms based on different assumptions.

Klinkenberg (1941) proposed the Klinkenberg slip model based on experimental data. A slip factor is defined to correct the slip effect on the permeability measurement. The permeability can be calculated by

$$k_a = k_0(1 + \frac{b}{\overline{p}}) \tag{3}$$

where k_a is gas permeability at mean pressure $\overline{p}$ in porous media, k_0 is intrinsic permeability of the sample. The b is an empirical parameter named as slip factor. We can find $k_a > k_0$ when $\overline{p}$ is small, and $k_a \to k_0$ when $\overline{p} \to \infty$. It is common to use the Klinkenberg effect to simulate the gas flow process in conventional gas reservoirs and some tight porous media gas systems.

Beskok and Karniadakis (1999) developed a model of the gas flow through a single pipe which was applicable in the entire Knudsen range. The permeability can be calculated by

$$k_a = \frac{r^2}{8} f(K_n) \tag{4}$$

$$f(K_n) = (1 + \overline{\alpha} K_n)(1 + \frac{4K_n}{1 - \overline{b} K_n}) \tag{5}$$

where r is pipe radius, $\overline{b}$ is slip coefficient which equals to -1 (Beskok and Karniadakis, 1999), the rarefaction coefficient $\overline{\alpha}$ can be determined by K_n and varied from 0 (slip flow) to α_0 (free molecule flow). Ziarani and Aguilera (2012) called $f(K_n)$ as Knudsen's correction factor and found the Knudsen's permeability correlation was more accurate than Klinkenberg's model especially in the flow regimes of transition and free molecular. The rarefaction coefficient $\overline{\alpha}$ can be calculated by

$$\overline{\alpha} = \alpha_0 \frac{2}{\pi} \tan^{-1}(\alpha_1 K_n^{\alpha_2}) \tag{6}$$

where $\alpha_1 = 4.0$, $\alpha_2 = 0.4$, and α_0 can be determined in the free molecule flow region by obtaining the asymptotic constant for the mass flow rate when Kn approaches infinity (Beskok and Karniadakis, 1999). The α_0 can be expressed with the slip coefficient $\overline{b}$ as follows:

$$\overline{\alpha}_{K_n \to \infty} \equiv \alpha_0 = \frac{64}{3\pi(1 - 4/\overline{b})} \tag{7}$$

Javadpour (2009) presented a gas transport model based on two major mechanisms of slip flow and Knudsen diffusion in a single, straight, cylindrical nanotube. By considering the Knudsen diffusion and the slip flow, the total mass flux through a nanopore is:

$$J = -\left(\frac{2rM}{3 \times 10^3 RT} \left(\frac{8RT}{\pi M} \right)^{0.5} + F \frac{r^2 \rho_a}{8\mu} \right) \frac{p_2 - p_1}{L} \tag{8}$$

where F is theoretical dimensionless coefficient which is defined to correct the slip velocity in tubes as (Brown et al., 1946):

$$F = 1 + \left(\frac{8\pi RT}{M} \right)^{0.5} \frac{\mu}{p_a r} \left(\frac{2}{\alpha} - 1 \right) \tag{9}$$

where M is gas molar mass, R is universal gas constant, μ is gas viscosity, ρ_a is average gas density, L is the length of the nanotube, and p_1 and p_2 are the pressures at the inlet and exit side of the pore, respectively. The p_a is average pressure of p_1 and p_2, and α is the tangential momentum accommodation coefficient which ranges from 0 to 1.

The apparent permeability formulation of the volumetric gas flux is:

$$k_a = \frac{2r\mu M}{3 \times 10^3 RT \rho_a^2} \left(\frac{8RT}{\pi M} \right)^{0.5} + F \frac{r^2}{8\rho_a} \tag{10}$$

Civan (2010) proposed a gas transport model based on Beskok and Karniadakis (1999) model and the assumption of a bundle of tortuous capillary tubes with the same diameters in porous media. The permeability formulation is a function of the intrinsic permeability k_∞, the Knudsen number K_n, the slip coefficient $\overline{b}$, and the rarefication coefficient $\overline{\alpha}$.

$$k = k_\infty (1 + \overline{\alpha} K_n)(1 + \frac{4K_n}{1 - \overline{b} K_n}) \tag{11}$$

$$k_\infty = \frac{\phi r^2}{8\tau} \tag{12}$$

where ϕ is the porosity of porous media, τ is the tortuosity factor of hydraulic preferential flow paths in porous media.

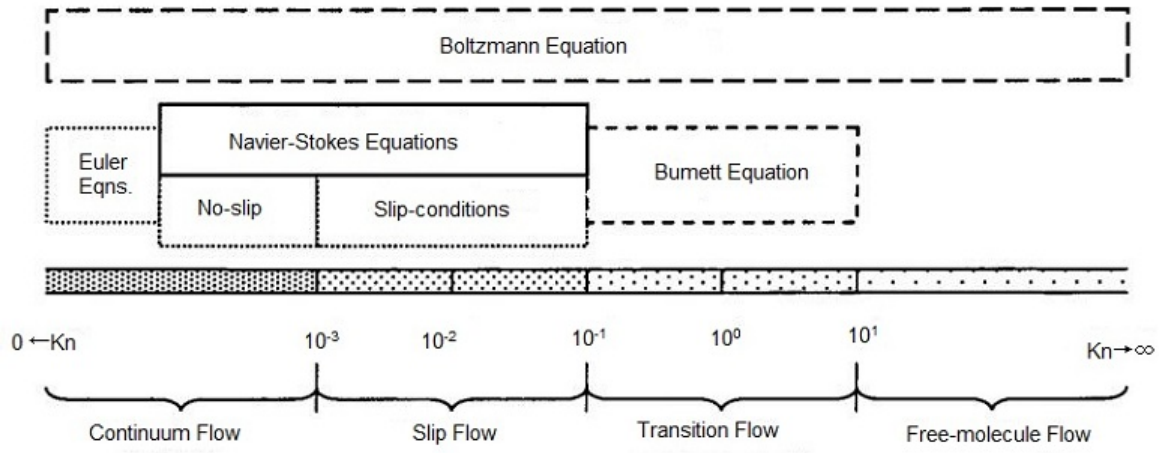

Fig. 2. Knudsen number regimes and different flow regimes (Roy et al., 2003).

The dimensionless rarefication coefficient $\overline{\alpha}$ is given by Civan (2010) as follows:

$$\frac{\alpha_0}{\overline{\alpha}} - 1 = \frac{A}{K_n^B}, \quad A > 0, B > 0 \tag{13}$$

where A and B are fitting parameters.

Darabi et al. (2012) proposed an apparent permeability function based on several modifications of the gas transport model of Javadpour (2009). They modified the model from a single straight cylindrical nanotube to ultra-tight natural porous media, which is considered the micropores and nanopores as tortuous capillary tubes.

$$k_a = \frac{2r\mu M}{3RT\rho_a}\frac{\phi}{\tau}(\delta')^{D_f-2}\left(\frac{8RT}{\pi M}\right)^{0.5} + F\frac{r^2}{8} \tag{14}$$

where δ' is the ratio of the normalized molecular radius size (r_m) to the local average pore radius (r_a), i.e., $\delta' = r_m/r_a$. The average pore radius r can be determined by laboratory experiments, such as mercury injection, SEM and AFM (Darabi et al., 2012).

There is a parameter, D_f, in the apparent permeability function by Darabi et al. (2012). The term D_f is the fractal dimension of pore surface which is defined to consider the effect of pore-surface roughness on the Knudsen diffusion coefficient (Coppens, 1999; Coppens and Dammers, 2006). There will be an increase in residence time of molecules in porous media and a decrease in Knudsen diffusivity when the increasing surface roughness happens (Darabi et al., 2012). D_f is a quantitative measure of the surface roughness varied between 2 and 3. The lower limit and upper limit represent smooth surface and space-filling surface, respectively (Coppens and Dammers, 2006). Darabi et al. (2012) found that the effects of slip flow and Knudsen diffusion were more pronounced at lower reservoir pressures.

The models of gas transport in tight reservoirs mentioned above did not consider the surface diffusion of adsorbed gas, the influence of real gas effect, non-circular cross section and some other influence factors in nanopores of shale gas reservoirs. Thus, we will introduce other gas transport models which account for the effects of coupling the different influence factors in the following section.

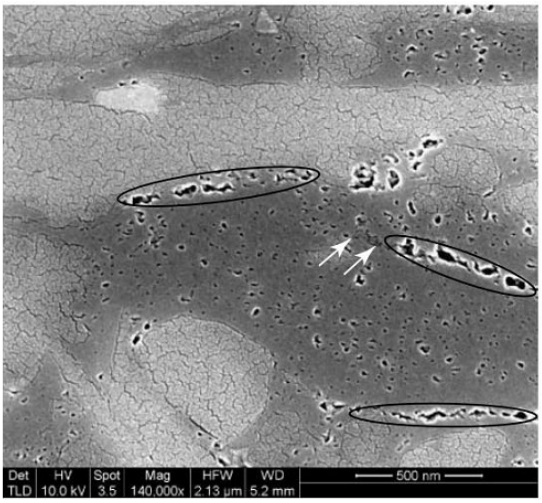

Fig. 3. Diverse cross-section types and shapes of nanopores (Milliken et al., 2013).

3. Complicated models with different effects included

Generanly, there are organic pores, inorganic pores and microcracks in the shale gas reservoirs. Milliken et al. (2013) found that pores within the organic matter were a significant component of pore systems in gas shales reservoirs. We can find some conclusions from SEM images of Javadpour et al. (2015) that the organic materials are amorphous with material type heterogeneities at small scale. In addition, we can find the diversity of nanopores in cross-section types and shapes from Figs. 3 and 4. The cross section in the nanopores are not always circular.

The organic matter with nanopores which is the media of gas storing and sourcing has a significant influence on the

gas transport in shale gas reservoirs (Wu et al., 2014, 2015b, 2015c). The apparent permeability of organic rich shale is complicated due to the coexisted adsorbed phase and free phase gases (Wang et al., 2016c).

Wu et al. (2014) made a comparison of different permeability models and proposed a new apparent permeability model which can accurately calculate the apparent permeability including the mechanisms of viscous flow, Knudsen diffusion, and desorption.

The bulk gas flux is a weighted summation based on their different contributions of viscous flow and Knudsen diffusion. The weighted factors for viscous flow and Knudsen diffusion are quantified by the ratio of collision frequency between molecules or collision frequency between nanopores wall and molecule to total collisions frequency, respectively (Wu et al., 2014). In addition, the bulk gas apparent permeability is also considered with the effects of rarefaction, nanopores structure, poromechancial and sorption-induced swelling response. The Langmuir isotherm equation and mass balance equation were used to study the effect of gas desorption. The final total permeability can be calculated by

$$k_a = \left(\frac{\phi}{\tau} \frac{r^2 p V_s (1+\overline{\alpha} K_n)}{8RT(1+K_n)} + \frac{V_s \mu}{(1+1/K_n)} \frac{2}{3} \frac{\phi}{\tau} r(\delta')^{D_f-2} \left(\frac{8}{\pi RTM} \right)^{0.5} \right) \omega_m \omega_s + \frac{\phi_a}{\phi} k_t \tag{15}$$

where k_t is the apparent permeability for bulk gas through shale nanopores, V_s is the mole volume of gas at standard temperature (273.15 K) and pressure (101,325 Pa) with the value of 22.414×10^{-3} $m^3 mol^{-1}$, ω_m is the poromechancial response coefficient of shale matrix, ω_s is the sorption-induced swelling response coefficient of shale matrix, ϕ_a is the effective adsorption porosity induced by adsorbed gas.

Wu et al. (2015c) proposed a new model based on Hwang model to discribe the surface diffusion for adsorbed gas in shale gas reservoirs. The surface diffusion model was considered with the effects of surface heterogeneity, isosteric sorption heat, and nonisothermal gas desorption. The final total permeability can be calculated by

$$k_a = \xi_s D_s \frac{C_s V_s \mu}{pM} + \xi_b \left(r^2 \frac{pV_s}{8RT} \frac{1+\overline{\alpha} K_n}{1+K_n} \left(1 + \frac{6K_n}{1-\overline{b} K_n} \right) + \frac{2r(\delta')^{D_f-2}}{3} \left(\frac{8}{\pi RTM} \right)^{0.5} \frac{K_n V_s \mu}{1+K_n} \right) \tag{16}$$

where ξ_s and ξ_b are the correction factors for the surface diffusion and the bulk gas transport in shale gas reservoirs, respectively. The term D_s is the gas surface diffusion coefficient, and C_s is the adsorbed gas concentration.

Wu et al. (2015a) also studied the real gas effect on gas transport in nanopores with different cross-section shapes in shale gas reservoirs. They found that both the type of cross-section and the shape of nanopores affected gas transport capacity.

Ren et al. (2016) proposed an analytical model for real gas transport in nanopores of shale reservoirs based on the linear superposition of convective flow and Knudsen diffusion. The model was established to be free of tangential momentum accommodation coefficient and taken into the effect of pore shape and real gas. The effect of pore shape on the gas flow properties in noncircular nanopores can be quantified with a more general paramete a $(a \geq 1)$ proposed by Cai et al. (2014). The intrinsic permeability can be calculated with the equivalent pore radius r by

$$k_d = \frac{\phi a^4 r^2}{8\tau} \tag{17}$$

The final total permeability can be calculated by

$$k_a = k_d \left(1 + \frac{\phi}{\tau} \frac{D_{kr} \overline{\mu}}{p k_d} \right) \tag{18}$$

where $\overline{\mu}$ is corrected viscosity, and D_{kr} is the Knudsen diffusion coefficient for real gas which can be calculated with the compressibility factor Z as follows:

$$D_{kr} = \frac{2}{3}(ar) \sqrt{\frac{8ZRT}{\pi M}} \tag{19}$$

Geng et al. (2016a) put forward a model for gas transport in nanopores based on the extended Navier−Stokes equations with the assumption of neglecting adsorption and desorption. The total mass flux was superimposed with a weighted superposition of bulk and Knudsen diffusion. The final total permeability can be calculated with the ratio coefficient b' by

$$k_a = \frac{r^2}{8} + \frac{K_n^{b'+1} + K_n}{K_n^{b'+1} + 1} \frac{2r}{3} \frac{\mu}{p} \sqrt{\frac{8RT}{\pi M}} \tag{20}$$

The term b' $(b' > 0)$ is the only parameter needed to be determined in the model. The value of 1 for b' is accurately determined by comparing the outcome of the DSMC method with the experimental data.

The permeability models mentioned above have considered the effects of surface diffusion of adsorbed gas, the real gas effect, non-circular cross section and some other effects.

4. Fractal gas permeability model of tight porous media

The multiscale feature and the structure of nanopores have significant effects on the permeability of shale. Researchers found that the pore surfaces of shale samples have fractal geometries (Yang et al., 2014; Liu et al., 2015; Sheng et al., 2016).

Yang et al. (2014) investigated the different influences of fractal characteristics of shales based on adsorption capacity of shale gas reservoirs in the Sichuan Basin, Chine. They found that the fractal dimensions of the shale samples ranging from 2.68 to 2.83, which can be used to evaluate the adsorption capacity. It will be significant to use the fractal analysis method to investigate fractal characteristics of shales and get a better understanding of the pore structure and adsorption capacity of shale gas reservoirs (Yang et al., 2014). There are

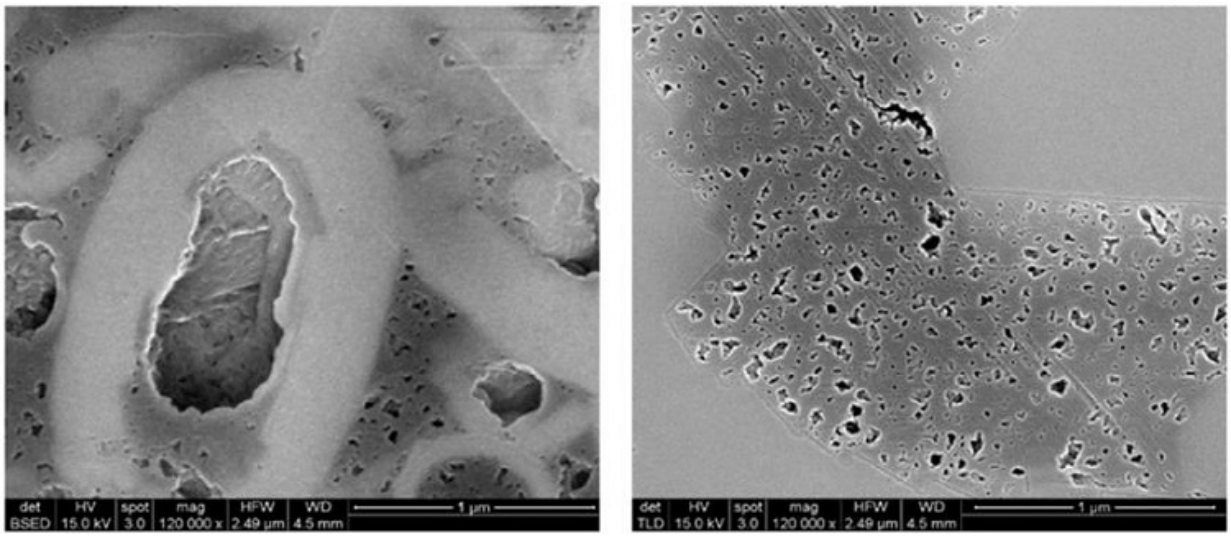

Fig. 4. Two exemplary SEM images of the pores in organic matter (Javadpour et al., 2015).

some researchers who have investigated fractal permeability model of gas transport in tight reservoirs based on the fractal theory.

Zheng et al. (2013) developed a fractal permeability model of gas transport in slip flow regime ($10^{-3} < K_n < 10^{-1}$) based on fractal theory. The apparent gas permeability can be calculated by parameters with definite physical meaning:

$$k_a = \frac{\pi D_p \lambda_{max}^{3+D_t}}{128 L_0^{D_t-1} A(3+D_t-D_p)} \left[1+\frac{8l(3+D_t-D_p)}{\lambda_{max}(2+D_t-D_p)}\right] \quad (21)$$

where D_p is the fractal dimension for pore spaces in range of $0 < D_p < 2$ and $0 < D_p < 3$ in two and three dimensional spaces, respectively. The term D_t is the fractal dimension for tortuosity which ranges from 1 to 2 (or 3) in two (or three) dimensions. The term L_0 is the straight length of capillary pathways along the flow direction, and A is the cross sectional area of a unit cell (Zheng et al., 2013).

The maximum pore diameter λ_{max} can be calculated with the expression introduced by Cai and Yu (2010)

$$\lambda_{max} = \sqrt{32\tau K_\infty \frac{4-D_p}{2-D_p}\frac{1-\phi}{\phi}} \quad (22)$$

Sheng et al. (2016) put forward a shale gas permeability model based on the model of Beskok and Karniadakis (1999) and the fractal theory with the effects of multiscale flow within a multiscale pore space. The apparent permeability can be computed from the sum of individual permeabilities which were the integral values of different flow regimes based on the assumption of independence of flow behaviors at multiscale pores.

$$k_a = \sum_{i=1}^{N} k_a^i \quad (23)$$

They simplified the pore structure as multiscale straight capillaries with D_t=1. The integral values of different flow regimes for individual permeabilities k_a^i can be calculated by when $K_n \le 0.1$,

$$k_a^i = \frac{\pi D_p \lambda_{i+1}^4}{128(4-D_p)A_i}\left[1-\left(\frac{\lambda_i}{\lambda_{i+1}}\right)^{4-D_p}\right] + \frac{8\pi D_p \lambda_{i+1}^3 l}{128(3-D_p)A_i}\left[1-\left(\frac{\lambda_i}{\lambda_{i+1}}\right)^{3-D_p}\right] \quad (24)$$

when $K_n \ge 10$,

$$k_a^i = D_p \lambda_{i+1}^{D_p} \cdot f(\lambda) \quad (25)$$

when $0.1 \le K_n \le 10$,

$$k_a^i = D_p \lambda_{i+1}^{D_p} \cdot g(\lambda) \quad (26)$$

where λ_i and λ_{i+1} are the minimum and maximum pore diameters at the corresponding diameter range for the ith interval, respectively. The term A_i is the cross sectional area of ith pore-size interval, and $f(\lambda)$ and $g(\lambda)$ are the complicated integral functions which have no analytical solutions. Because of the limitation of current articals, we have not given the formulas of $f(\lambda)$ and $g(\lambda)$. The interested reader can refer to the article of Sheng et al. (2016).

Yuan et al. (2016b) proposed an apparent permeability incorporated with porous flow and surface diffusion based on the model of Beskok and Karniadakis (1999) and Langmuir isotherm absorption model (Langmuir, 1918). The model can be calculated with a assumption that the porous structure was representd as a boundle of tortuous capillary tubes with different diameters based on fractal theory. The final total permeability can be calculated by

$$k_a = \frac{L_0^{1-D_t}(2-D_p)}{\lambda_{max}^{2-D_p}-\lambda_{min}^{2-D_p}}\left[\frac{\phi}{32}\int_{\lambda_{min}}^{\lambda_{max}} \lambda^{2-D_p+D_t} f(K_n) d\lambda + \frac{(1-\phi)\overline{D}_{s,0}}{1+\hat{b}p}\frac{\hat{b}C_L M}{\rho_a \mu^{-1}}(\lambda_{max}^{1-D_p+D_t}-\lambda_{min}^{1-D_p+D_t})\right] \quad (27)$$

where λ_{min} is the minimum pore sizes, $\overline{D}_{s,0}$ is the surface diffusivity at zero loading, $\hat{b}$ is the Langmuir constans defined as the reciprocal of Langmuir pressure p_L, and C_L is the maximum adsorption capacity at constant temperature and infinitely high pressure (Yuan et al., 2016b).

Geng et al. (2016b) thought the real gas flow in a single pore based on the previously reported Extended Navier-Stokes Equations method (Geng et al., 2016a). The modified mass flow rate of free gas M^f and adsorbed gas M_r^s in variably shaped pores can be calculated by

$$M^f = -\left[\frac{a^2\lambda^2}{32\hat{\mu}}\frac{pM}{ZRT} + \frac{K_n^2+K_n}{K_n^2+1}\frac{a\lambda}{3}\sqrt{\frac{8ZM}{\pi RT}}\left(\frac{1}{Z}-\frac{p}{2Z^2}\frac{\partial Z}{\partial p}\right)\right]\frac{\pi a^2\lambda^2}{4}\partial_x p \tag{28}$$

$$M_r^s = -\overline{D}_{s,0}MC_L\left[\frac{1}{Zp_L+p} - \frac{p}{Z(Zp_L+p)}\frac{\partial Z}{\partial p}\right]\pi(a\lambda\lambda_r-\lambda_r^2)\partial_x p \tag{29}$$

where $\hat{\mu}$ is the viscosity depending on the pressure and temperature, and λ_r is the thickness of a single layer for the adsorbed gas molecules with the consideration of gas compressibility factor (Geng et al., 2016b).

The apparent permeability of organic and inorganic matter cells were caltulated with fractal theory concepts. In addition, the apparent permeability was upscaled to the sample scale with the consideration of heterogeneous distribution of organic matter. Because the calculation formula of fractal apparent permeability is too long and the limited space, the fractal calculation formula are not given in this artical. The interested reader can refer to the article of Geng et al. (2016b).

Behrang and Kantzas (2017) used a hybrid methodology with combination of fractal theory, kinetic theory of gases and Boltzmann transport equation to predict the gas permeability in nanoscale organic materials. The total gas mass flux can be calculated by

$$J_{total} = \frac{\phi}{\tau}[\xi J_{vis} + J_{surf} + (1-\xi)J_{K_n}] \tag{30}$$

where J_{vis}, J_{surf}, J_{K_n} are viscosity, surface diffusion and Knudsen mass flow rates, respectively. The term ξ is the ratio of intermolecular collision frequency to total collisions frequency (Thompson and Owens, 1975; Sheng et al., 2015). The conception of calculation for ξ is the same as that of the weighted factor of viscous flow by Wu et al. (2014).

$$\xi = \frac{1}{1+K_n} \tag{31}$$

The absolute permeability k_0' of viscous flow was calculated using the modified fractal theory by

$$k_0' = \frac{(\pi D_p)^{(1-D_t)/2}(4(2-D_p))^{(1+D_t)/2}}{64(3+D_t-D_p)}a_p^2\left(\frac{\phi_e}{1-\phi_e}\right)^{(3+D_t)/2} \tag{32}$$

where a_p is the grain size, and ϕ_e is the effective porosity considered adsorption layer thickness d_a by

$$\phi_e = \phi\left(1-\frac{d_a}{r}\right)^2 \tag{33}$$

The gas permeability can increase when the grain surface specularity rises, but this effect could be negligible at high pressure regions. The final total permeability expression can be calculated by

$$k_{total} = \frac{\phi}{\tau}\left(\xi k_0' + \frac{\rho_s}{\rho_g}D_s'\mu\frac{p_L}{(p+p_L)^2} + (1-\xi)\frac{\mu}{p}D_K'\right) \tag{34}$$

where ρ_s is adsorbed gas density, ρ_g is gas density, D_s' is the complicated surface diffusion coefficient, and D_K' is the self-diffusivity mass transfer coefficient. The interested reader can refer to the article by Behrang and Kantzas (2017) to find the expressions of D_s' and D_K'.

We can find that the apparent permeability can be upscaled from an ideal single capillary to the sample scale with different considerations of real gas effect based on fractal theory. In addition, the expression for apparent permeability of shale gas sample has parameters with clear physical meaning.

Because of highly anisotropic and heterogeneous of structure in shale gas reservoirs, some researchers used other methods to investigate the permeability of shale gas. Wang et al. (2016d) reconstructed 3D structure of shale sample based on the Quartet Structure Generation Set (QSGS) method and used lattice Boltzmann method (LBM) to predict the intrinsic permeability and apparent permeability. They also established the quantitative relationship between geometry features and gas permeability.

The principles of gas transport in nanoscale pores are complicated. However, we can use the kinetic theory of gases, fractal theory, Boltzmann transport equation and other methods to predict gas permeability in shale reservoirs.

5. Dynamic gas production process in shale

Considerable gas transport and storage models have also been proposed, in which the processes of gas diffusion and adsorption are considered (Fathi and Akkutlu, 2009; Freeman et al., 2011). Javadpour et al. (2007) included the Knudsen mechanism into the gas diffusion model for shale, in which condition, the flow channel has close diameter as the mean free path of the gas molecules. Freeman et al. (2011) and Yao et al. (2013) mixed the diffusion mechanisms through dusty gas model (DGM). Through the Knudsen number, Civan (2010) coupled the Knudsen diffusion and the viscous diffusion during gas production. Wu et al. (2016) calculated the contributions of viscous flow and Knudsen diffusion, by considering the colliding probabilities of gas molecules with each other and with nanopore walls. Yang et al. (2016b) and Wang et al. (2017) show in their paper a model considering the effect of adsorption/desorption on gas transport.

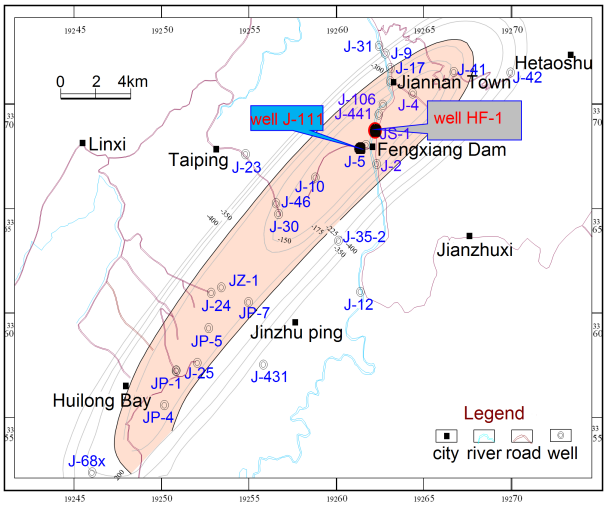

Fig. 5. Geologic map for shale in Sichuan Basin (Wang et al., 2016a).

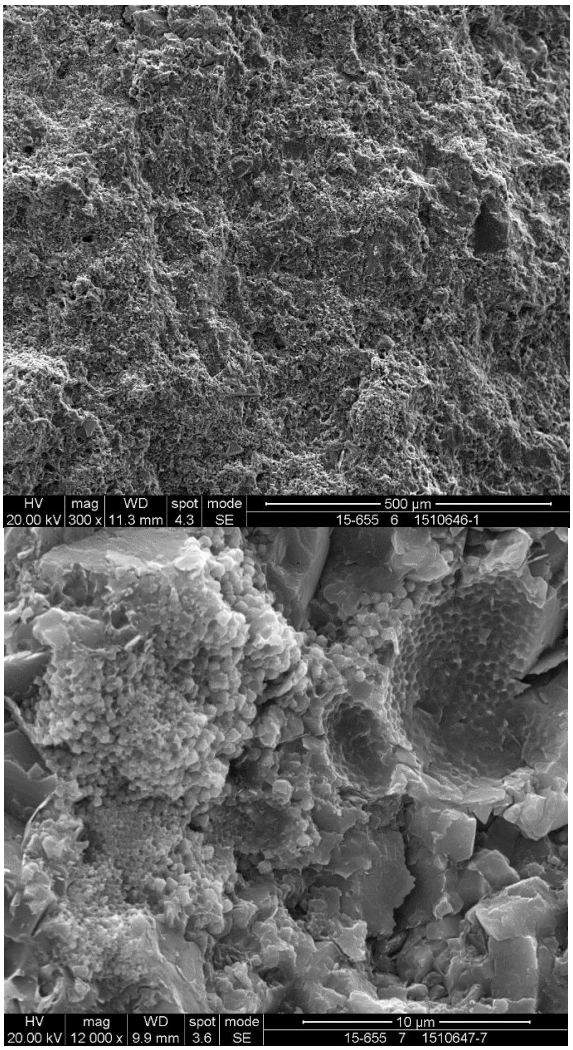

Fig. 6. SEM images for the shale sample.

5.1 Characterization of shale

The shale investigated here are collected from Silurian age of Lower Jurassic Formation, in Sichuan fold belt, China. The Geologic map is shown in Fig. 5. The samples tested in this paper were collected from well HF-1, as indicated in the center. The samples were obtained from depths between 585 and 643 m, with formation thickness of more than 100 m. The particles used in this section are assumed to be spheres, with an average diameter of 1,180 μm.

Fig. 6 shows the SEM (Scanning electron microscopy) images of the shale sample. SEM could intuitively and qualitatively describe the pores in shale and give the rough order of the pore size. Obviously, there distributes considerable amount of organic material among the inorganic matter, making shale pores complex. Haber (1991) classified pores into three types by their pore size: micropores ($<$ 2 nm), mesopores (2$\sim$50 nm), and macropores ($>$ 50 nm). Gas stores in micropores/mesopores mostly as adsorbed gas, while in mesopores/macropores as free gas. Another observation from Fig. 6 is that, there are many micropores/mesopores existed in the organic matter, which provides large surface for the gas adsorption.

5.2 Dynamic gas transport model

More than one gas transport mechanisms coexist in shale rocks during production. An equation considering the effect of adsorption/desorption and diffusion is developed to describe this gas production process for accurate field application. The share of free gas and adsorbed gas is investigated. Hence, based on the knowledge of adsorbed gas adsorption/desorption from kerogen and free gas flow in pores, we define the adsorption rate coefficient (λ'), desorption rate coefficient (μ') and apparent gas diffusion coefficient (D) in this study. According to this consideration, the controlling equation of the numerical model is (Wang et al., 2017; Yang et al., 2016b)

$$\frac{\partial c_f}{\partial t} = D\left(\frac{\partial^2 c_f}{\partial r^2} + \frac{2}{r}\frac{\partial c_f}{\partial r}\right) - \frac{\partial c_a}{\partial t} \tag{35}$$

where c_f is the free gas concentration in the pore space of the shale particle, r is the distance to the center of the shale particle, c_a is the equivalent surface concentration or adsorbed gas concentration, and t is time.

The following equation exhibits the dynamic gas adsorption/desorption process before equilibrium,

$$\frac{\partial c_a}{\partial t} = \lambda' c_f - \mu' c_a \tag{36}$$

In Eq. (36), when $\lambda' \times c_f$ is smaller than $\mu' \times c_a$, the gas in kerogen starts to produce. Parameters λ' and μ' satisfy the following equation,

$$\frac{\lambda'}{\mu'} = R' = \frac{c_a^{eq}}{c_f^{eq}} \tag{37}$$

where c_a^{eq} is the equilibrium concentration of the adsorbed gas concentration on the surface, c_f^{eq} is the equilibrium free gas

concentration in the pore space, and R' is the ratio as indicated by Eq. (37).

With constant boundary conditions and the initial conditions, the analytical solutions for the free gas concentration (c_f) and equivalent surface concentration (c_a) of adsorbed gas are equal to

$$c_f = c_{f0} + \sum_{n=1}^{\infty} \frac{(c_{f0} - c_{fi}) e^{p_n t} \sin(m_n r)}{\frac{r\sin(m_n r_0)}{r_0} - \frac{p_n r}{2m_n D}\left(1 + \frac{\lambda' \mu'}{(p_n + \mu')^2}\right)\cos(m_n r_0)} \quad n = 1, 2, 3 \tag{38}$$

$$c_a = c_{a0} + \sum_{n=1}^{\infty} \frac{(c_{a0} - c_{ai}) \mu' e^{p_n t} \sin(m_n r)(p_n + \mu')^{-1}}{\left(-\frac{p_n r}{2m_n D}\left(1 + \frac{\lambda' \mu'}{(p_n + \mu')^2}\right)\cos(m_n r_0) + \frac{r\sin(m_n r_0)}{r_0}\right)} \tag{39}$$

The total gas produced then can be obtained accordingly.

5.3 Effect of temperature and pressure

The adsorbed gas and free gas production dynamic are studied experimentally and mathematically. Besides, the effect of temperature and pressure on the gas production process is explored in detail in this section.

Higher temperature can decrease the total gas production and take less time for obtaining the equilibrium, as shown in Fig. 7. For higher temperature, it makes the diffusion coefficient and surface diffusion coefficient larger, thus leading to faster gas mass transport. The surface coverage of methane drops when the temperature increases, which could explain the decreasing trend of V_t with increasing temperature in Fig. 7. Another, the physical adsorption of molecules to the surface becomes weak at higher temperatures because of the weaker physisorption. The contribution of the desorbed gas on gas production differs at different temperatures.

Fig. 8 shows the pressure effect on the gas flow process in shale. Clearly shown is that the total production V_t increases with rising pressure. However, V_t increased nonlinearly with the test pressures. The reasons probably are: firstly, the compressibility factor. For similar pressure differential and pore volume, the produced free gas amount declines with increasing pressure. Secondly, the adsorption isotherm curve indicates that the adsorbed gas amount share the same tendency as the free gas with respect to pressure. Therefore, the incremental amount of V_t drops with rising pressure. Another, obtaining the equilibrium takes less time for tests at higher pressure. Additional attempts was made to study the gas transport dynamic by testing with He and CH_4. Tests results show that, adsorbed gas affects the gas transport in nanopores of shale by increasing the capacity of the gas production and changing the velocity of gas mass transport. For the tested shale sample, the adsorbed gas increases the gas mass transport and enhances the capacity of the total gas production by more than 3 times compared with the free gas transport. This value could be higher when utilizing shale with higher TOC. Besides, with the adsorbed phase in the surface of inner pores, surface diffusion is expected to enhance the dynamic gas flow process.

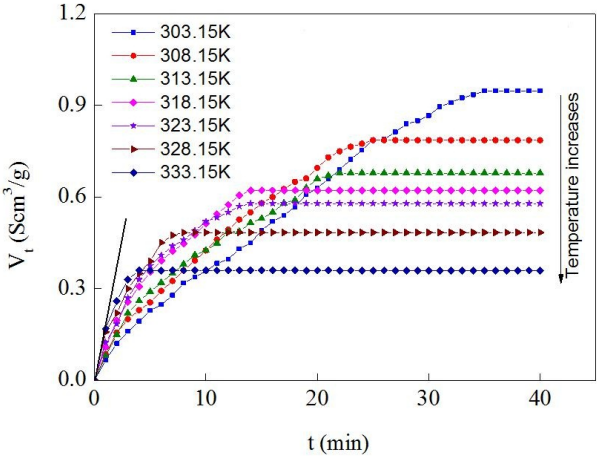

Fig. 7. Effect of temperature on the total mass production of methane in shale (Wang et al., 2017).

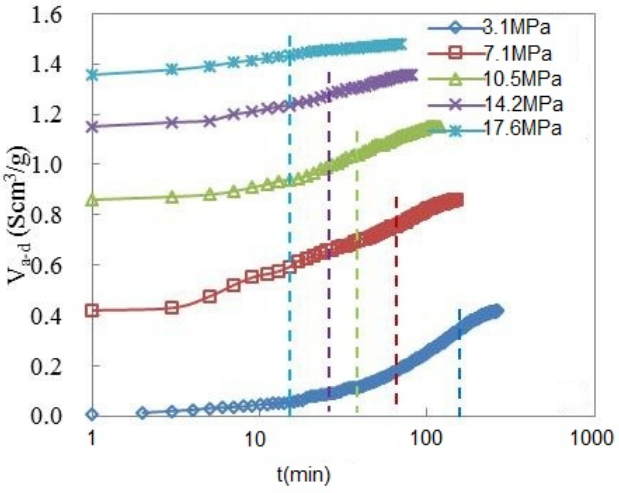

Fig. 8. Effect of pressure on the CH4 mass transport in shale sample (Wang et al., 2016b).

6. Gas production

6.1 Contribution of adsorbed gas on gas production

Contributions of free gas and adsorbed gas to the total gas production are calculated and discussed with the mathematical model presented in section 5. Fig. 9 presents the production of free gas and adsorbed gas with respect to time and their corresponding production rates. As can be seen, both adsorbed gas and free gas contribute to the total gas production. But for the last stage, after 11 min, the adsorbed gas contributes more to the total gas production. This could explain the fact in shale field that, the production for a shale well decreases sharply at beginning but produces at a relatively low rate for a long period. For adsorbed gas, the surface diffusion in shale is also studied. The surface diffusion coefficient is as low as 10^{-16} m^2/s, four orders of magnitude smaller than the Knudsen diffusion coefficient and six smaller than

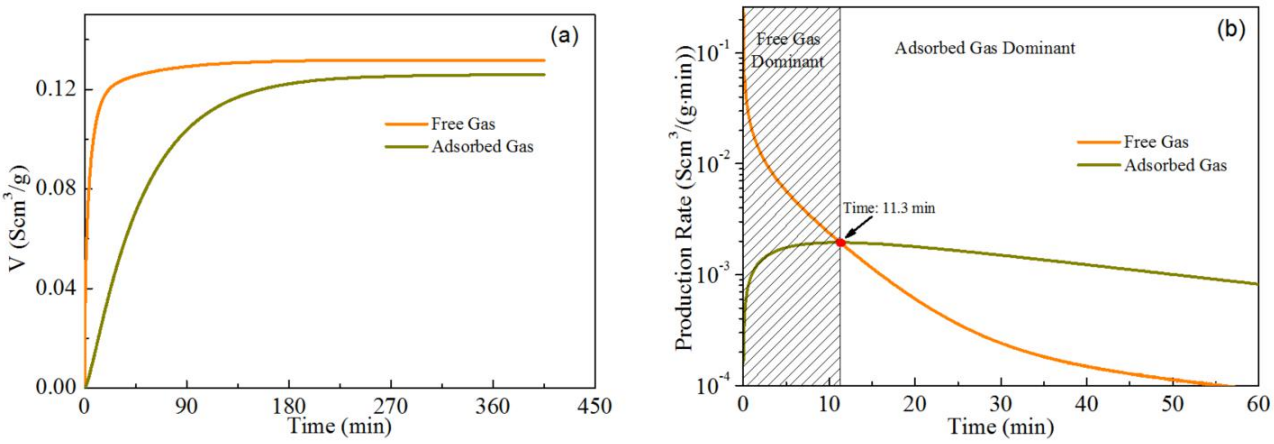

Fig. 9. Simulated results of (a) the cumulative productions and (b) the production rates of free gas and adsorbed gas for the transport process of CH4 at 3.4 MPa and 308 K (Wang et al., 2016a).

the apparent diffusion coefficient. It has been stated that the surface diffusion should be accounted for the late stage of the gas production. Mathematical calculation and experimental tests reveal that the surface diffusion can enormously promote the gas transport process, even the diffusion coefficient is very low compared with the free gas diffusion coefficient. Accurate prediction of the diffusion coefficient is important for evaluating a reservoir and forecasting the field production.

6.2 Contribution of unstimulated reservoirs outside SRV

Flow-regimes have been identified and studied extensively for multi-fractured horizontal wells (MFHW) in shale plays (Cheng, 2011; Song et al., 2011). In addition, in view of ultra-low permeability, transient linear flow is the dominate flow regime in tight/shale plays, which can continue for several years. As reported by Clarkson (2013), the majorities of hydrocarbon production are attributed to the stimulate-dreservoir volume, (SRV, referred to dynamic drainage volume (DDV) corresponding to the end of transient-linear flow) in ultra-low/shale reservoirs. Moghanloo et al. (2015) defined an asymptotic equation of DDV and within which average pressure, and applied an iterative algorithm to find their explicit formulation. Behmanesh et al. (2015) and Clarkson and Qanbari (2016a, 2016b) defined a new formula of distance-of-investigation only applicable for early transient-linear flow within SRV, but ignored the contributions of outer reservoirs to the long-term shale production. However, for the longterm production in shale, the flow regime would become compound-linear flow or else with an expanding production region in outer reservoirs. As results, the assumption of only transient linear flow in shale makes the material-balance model with SRV as the maximum size of DDV. Hence, it is desirable to account for the contributions of outer reservoirs into production data analysis. Yuan et al. (2016a) applied new mechanistic formula of Dynamic-Drainage-Volume applicable for both early transient-linear flow and late compound-linear flow regime, specific to multi-stage fractured horizontal wells (MFHW), and predicate the ultimate recovery of MFHW after long-term production. In Niobrara shale oil, the contribution of outer matrix outside SRV to the production is small but nonnegligible, approximately 3.5% after 3 years' production (Yuan et al., 2016a).

6.3 Gas recovery by spontaneous imbibition

Large volume fracturing fluids are pumped into formation during the shale gas development. The flow-back rate is generally lower than 30%, and even less than 5% (Penny et al., 2006; King, 2012). There is severe spontaneous imbibition of fracturing fluids from hydraulic fractures to matrix. Spontaneous imbibition is regarded as one important mechanism influencing the production after fracturing. The interaction between fluids and shale formation affects the production largely (Palisch et al., 2010; Soliman et al., 2012). Due to the significant mobility difference between gas and water, spontaneous imbibition usually causes gas reservoir damage based on the conventional theory of water blockage, especially in unconventional reservoirs with extremely small pores with strong capillary pressure (Bennion and Thomas, 2005; Roychaudhuri et al., 2013; Odumabo and Karpyn, 2014). However, spontaneous imbibition of shale has been paid serious attentions and is treated as one important potential mechanism for gas recovery in same cases (Cai et al., 2010, 2017; Yaich et al., 2015; Shen et al., 2016a). Fig. 10 shows the simulation results that the water imbibition through well shut-in can reduce the water saturation beside the fracture after hydraulic fracturing, which will benefit the production (Bertoncello et al., 2014). Spontaneous imbibition conducts different influence to gas production.

The imbibition characteristic of shale is different from ordinary sandstone according to the experiments. Imbibition rate was higher when parallel to the bedding plane, compared with the perpendicular direction. Besides, water will imbibe into the matrix from the fracture (Makhanov et al., 2012). Roychaudhuri et al. (2013) noted that the addition of surfactant could effectively change the wettability of shale and reduce the

Table 2. The evaluated and predicated performance of 10 fractured wells in Niobrara shale oil play (Yuan et al., 2016a).

Parameters	MFHW #1	MFHW #2	MFHW #3	MFHW #4	MFHW #5
Lateral length of horizontal well, ft	4,003	4,475	4,027	6,230	3,474
Number of fracture cluster, number	48	69	74	157	57
Stimulated-reservoir volume (SRV), 10^4 ft^3	8,927	8,995	9,504	1,4578	7,782
Average permeability within SRV, mD	0.0004	0.0003	0.0002	0.0001	0.0004
Estimated fracture half-length, ft	223	201	236	234	224
Maximum drainage volume, (MDV), 10^4 ft^3	11,388	18,890	11,959	18,681	10,011
Ultimate recovery factor (URF), percentage	7.21	10.34	7.96	6.39	7.91
Parameters	MFHW #6	MFHW #7	MFHW #8	MFHW #9	MFHW #10
Lateral length of horizontal well, ft	6,400	4,000	4,380	4,152	4,914
Number of fracture cluster, number	80	140	74	57	75
Stimulated-reservoir volume (SRV), 10^4 ft^3	11,776	9,386	9,373	8,802	11,459
Average permeability within SRV, mD	0.0003	0.00006	0.0002	0.0004	0.0004
Estimated fracture half-length, ft	243	247	214	212	233
Maximum drainage volume, (MDV), 10^4 ft^3	17,309	18,765	19,348	11,452	14,686
Ultimate recovery factor (URF), percentage	9.45	5.87	10.76	9.82	10.25

water intake rate and quantity. Shen et al. (2016a) conducted imbibition experiments using marine and continental shales. Liquid imbibition capacity and liquid diffusion ability are proposed to describe and compare the imbibition features, which indicated that shale has stronger water imbibition and diffusion capacity than relatively higher permeability sandstone, and marine shale has stronger water imbibition capacity than continental shale. Yang et al. (2016a) indicated that the water imbibition capacity is partially dependent on the clay mineral content and type, especially the amount of smectite and illite/smectite mixed-layer clay.

Capillary pressure is recognized as the main driving force for spontaneous imbibition by classic flow theory (Cai and Yu, 2012; Cai et al., 2014). The capillary force in unconventional gas reservoirs is significantly high because of the wide distribution of nanoscale pores and the ultra-low initial water saturation (Shen et al., 2016b). Clay effect is another important driving force for spontaneous imbibition. Dehghanpour et al. (2013) mentioned the water adsorption on the clay surface as a mechanism for water imbibition of shale. Fakcharoenphol et al. (2014) studied the effects of salinity on water imbibition and concluded that osmotic pressure acts as an important driving force to imbibition. In clay-rich shale, the osmotic pressure is more powerful than the capillary pressure, and the water volume imbibed into the matrix therefore significantly surpasses the pore volume measured by gas (Ge et al., 2015). Ghanbari et al. (2013) conducted imbibition/diffusion experiments and found that the imbibition curves are well correlated to that of diffusion curves. It shows that samples with rich clays and micro-fractures have higher ion diffusion rate. A series of imbibition/diffusion experiments on organic shale samples were conducted by Yang et al. (2017) and it is proposed that the imbibition fluid conductivity resulting from ion diffusion is proportional to the square root of time, which is similar to the law of capillary-driven imbibition into porous media. Based on the tortuous capillary model and fractal geometry, Cai et al. (2010, 2011) discussed the effect of tortuosity on the capillary imbibition in wetting porous media, modified the classical Lucas-Washburn equation and found that the imbibition time exponent is not 0.5, but is related to the tortuosity fractal dimension for streamlines.

The liquid distribution and mirco-migration during shale imbibition process are critical to gas production. Amplitude difference, vertex value, vertex position and peak width of T2 spectrum of the nuclear magnetic resonance technique can be useful to characterize the direction, speed and scope of the aqueous phase migration in rock samples. Meng et al. (2015a) indicated that the liquid filled into the small pores preferentially and then the larger pores in the left peak of shale T2 spectrum. Shen et al. (2017) introduced the magnetic resonance signals for different shale samples (Fig. 11). The signals are tests with the water imbibition. In Fig. 11, the water enters into the larger pores after 347 min.

The micro-fracture generation is a crucial factor for a high gas production after shale reservoir shut-in for a period of time (Wang et al., 2011). The additional driving force caused the excess water imbibition from water adsorption by clay minerals in shales and the increase of rock permeability by adsorption-induced micro-fractures (Dehghanpour et al., 2013). The shale with high clay content was prone to conducting micro-fractures and sample disintegration after sample imbibition. The permeability variation has been researched during imbibition with shale samples completely soaking into distilled water and it showed that both permeability increasing interval and decreasing interval appeared (Meng et al., 2015b).

The spontaneous imbibition tests and APT-NMR technique (aqueous phase trapping (APT) auto-removal combined with the low-field nuclear magnetic resonance (NMR)) could be

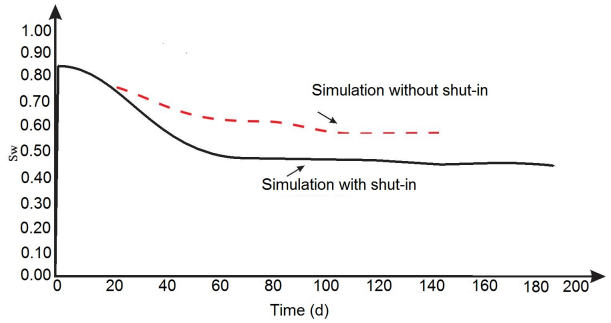

Fig. 10. Comparison of water saturation in the closest block to the fracture.

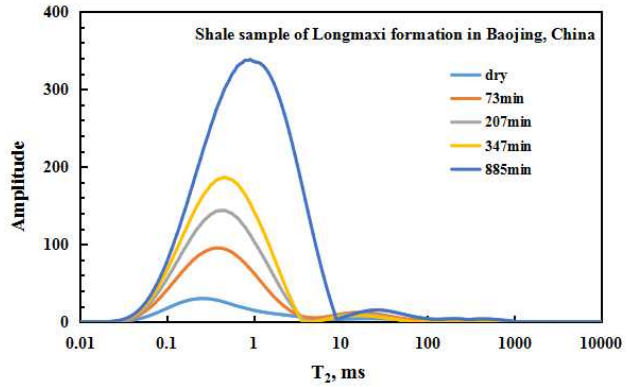

Fig. 11. NMR monitoring of the imbibition process for shale sample (Shen et al., 2017).

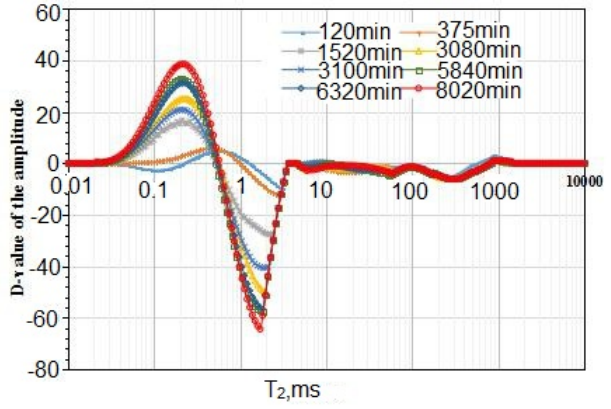

Fig. 12. D-value of the amplitude for shale in the water diffusion stage (Liu et al., 2016a).

used to study the mechanism of the APT auto-removal in shale. In the process of spontaneous imbibition, observations indicate that new pores were shown in shale samples, and the micro-cracks increased gradually on the sample surface (Meng et al., 2016). Liu et al. (2016a) put forward that aqueous phase migration between pores of different size has two stages based on the NMR monitor during water imbibition: in first stage, aqueous phase migrates from small pores to large pores; in second stage, it migrates from large pores to small pores, which decreases the water saturation in large pores. The duration and migratory volume of each stage are closely related to the pore characteristics and clay. This kind of experiment is helpful to understand the micro-imbibition process of shale (Fig. 12).

7. Conclusions

In this work, recent advances on gas flow and recovery in unconventional porous rocks are summarized and reviewed. Both mathematical models and the experimental results are listed and discussed. The most obvious factors influencing the gas flow process and the reservoir recovery include the permeability, adsorbed gas dynamics, stimulated reservoir volume/the unstimulated reservoir volume and the imbibition. Effects of adsorbed gas on the gas production process as well as the reservoir conditions are studied experimentally. The main conclusions are listed below:

1) Some basic models for gas transport in tight reservoirs have been summarized to study different factors of flow mechanisms based on different assumptions. In addition, several complicated models with different effects have been introduced with the considerations of complicated situations. The fractal gas permeability model of tight porous media can be obtained from an ideal single capillary to the sample scale with clear physical meaning parameters based on fractal theory.
2) Experimental results showed that, the dynamic adsorption process and the content of adsorbed gas both will influence the gas flow and recovery in unconventional porous rocks. Higher temperature will enhance the dynamic adsorption process but decrease the total adsorbed gas amount. The contribution of adsorbed gas to the total gas flowing into shale declined with temperature. Effect of kerogen content in shale should be fully considered for the gas flow and recovery process.
3) Even though imbibition cause gas reservoir damage based on the conventional theory of water blockage, it's positive effect on the shale gas recovery appears to be more and more important. Capillary pressure and clay effect are two main driving forces for spontaneous imbibition, mainly due to the wide distribution of nanoscale pores and the ultra-low initial water saturation.

Acknowledgments

YZ acknowledges the support from The Royal Society International Exchanges Scheme-China (NSFC) Joint Project.

References

Behmanesh, H., Clarkson, C.R., Tabatabaie, S.H., et al. Impact of distance-of-investigation calculations on rate-transient analysis of unconventional gas and light-oil reservoirs: New formulations for linear flow. J. Can. Pet. Technol. 2015, 54(6): 509-519.

Behrang, A., Kantzas, A. A hybrid methodology to predict gas permeability in nanoscale organic materials; a combination of fractal theory, kinetic theory of gases and Boltzmann transport equation. Fuel 2017, 188: 239-245.

Bennion, D.B., Thomas, F.B. Formation damage issues impacting the productivity of low permeability, low initial water saturation gas producing formations. J. Energy Res. Technol. 2005, 127(3): 240-247.

Bertoncello, A., Wallace, J., Blyton, C., et al. Imbibition and water blockage in unconventional reservoirs: Well-management implications during flowback and early production. Spectra Anal. 2014, 17(4): 497-506.

Beskok, A., Karniadakis, G.E. A model for flows in channels, pipes, and ducts at micro and nano scales. Microscale Thermophys. Eng. 1999, 3(1): 43-77.

Brown, G.P., DiNardo, A., Cheng, G.K., et al. The flow of gases in pipes at low pressures. J. Appl. Phys. 1946, 17(10): 802-813.

Bustin, A.M.M., Bustin, R.M. Importance of rock properties on the producibility of gas shales. Int. J. Coal Geol. 2012, 103: 132-147.

Cai, J., Ghanbarian, B., Xu, P., et al. Virtual special issue: Advanced theoretical and numerical approaches and applications to enhanced gas recovery. J. Nat. Gas Sci. Eng. 2017, 37: 579-583.

Cai, J., Yu, B. Advances in studies of spontaneous imbibition in porous media. Adv. Mech. 2012, 42(6): 735-754.

Cai, J.C., Perfect, E., Cheng, C.L., et al. Generalized modeling of spontaneous imbibition based on Hagen-Poiseuille flow in tortuous capillaries with variably shaped apertures. Langmuir 2014, 30(18): 5142-5151.

Cai, J.C., Yu, B.M. Prediction of maximum pore size of porous media based on fractal geometry. Fractals 2010, 18(4): 417-423.

Cai, J.C., Yu, B.M. A discussion of the effect of tortuosity on the capillary imbibition in porous media. Transp. Porous Media 2011, 89(2): 251-263.

Cai, J.C., Yu, B.M., Zou, M.Q., et al. Fractal characterization of spontaneous co-current imbibition in porous media. Energy Fuels 2010, 24(3): 1860-1867.

Chen, S., Zhu, Y., Wang, H., et al. Shale gas reservoir characterisation: A typical case in the southern Sichuan basin of China. Energy 2011, 36(11): 6609-6616.

Cheng, Y. Pressure transient characteristics of hydraulically fractured horizontal shale gas wells. Paper SPE 149311 Presented at the SPE Eastern Regional Meeting, Columbus, Ohio, USA, 17-19 August, 2011.

Civan, F. Effective correlation of apparent gas permeability in tight porous media. Transp. Porous Media 2010, 82(2): 375-384.

Clarkson, C.R. Production data analysis of unconventional gas wells: Review of theory and best practices. Int. J. Coal Geol. 2013, 109: 101-146.

Clarkson, C., Qanbari, F. A semi-analytical method for forecasting wells completed in low permeability, undersaturated CBM reservoirs. J. Nat. Gas Sci. Eng. 2016a, 30: 19-27.

Clarkson, C.R., Qanbari, F. History matching and forecasting tight gas condensate and oil wells by use of an approximate semianalytical model derived from the dynamic-drainage-area concept. SPE Reserv. Eval. Eng. 2016b, 19(4): 540-552.

Coppens, M.O. The effect of fractal surface roughness on diffusion and reaction in porous catalysts-from fundamentals to practical applications. Catal. Today 1999, 53(2): 225-243.

Coppens, M.O., Dammers, A.J. Effects of heterogeneity on diffusion in nanopores-from inorganic materials to protein crystals and ion channels. Fluid Phase Equilib. 2006, 241(1-2): 308-316.

Curtis, M.E., Ambrose, R.J., Sondergeld, C.H. Structural characterization of gas shales on the micro-and nano-scales. Paper SPE 137693 Presented at the Canadian Unconventional Resources and International Petroleum Conference, Calgary, Alberta, Canada, 19-21 October, 2010.

Darabi, H., Ettehad, A., Javadpour, F., et al. Gas flow in ultra-tight shale strata. J. Fluid Mech. 2012, 710: 641-658.

Dehghanpour, H., Lan, Q., Saeed, Y., et al. Spontaneous imbibition of brine and oil in gas shales: Effect of water adsorption and resulting microfractures. Energy Fuels 2013, 27(6): 3039-3049.

Etminan, S.R., Javadpour, F., Maini, B.B., et al. Measurement of gas storage processes in shale and of the molecular diffusion coefficient in kerogen. Int. J. Coal Geol. 2014, 123: 10-19.

Fakcharoenphol, P., Kurtoglu, B., Kazemi, H., et al. The effect of osmotic pressure on improve oil recovery from fractured shale formations. Paper SPE 168998 Presented at the SPE Unconventional Resources Conference, The Woodlands, Texas, USA, 1-3 April, 2014.

Fathi, E., Akkutlu, I.Y. Matrix heterogeneity effects on gas transport and adsorption in coalbed and shale gas reservoirs. Transp. Porous Media 2009, 80(2): 281-304.

Freeman, C.M., Moridis, G.J., Blasingame, T.A. A numerical study of microscale flow behavior in tight gas and shale gas reservoir systems. Transp. Porous Media 2011, 90(1): 253-268.

Ge, H.K., Yang, L., Shen, Y.H., et al. Experimental investigation of shale imbibition capacity and the factors influencing loss of hydraulic fracturing fluids. Pet. Sci. 2015, 12(4): 636-650.

Geng, L., Li, G., Zitha, P., et al. A diffusion-viscous flow model for simulating shale gas transport in nano-pores. Fuel 2016a, 181: 887-894.

Geng, L.D., Li, G.S., Zitha, P., et al. A fractal permeability model for shale gas flow through heterogeneous matrix systems. J. Nat. Gas Sci. Eng. 2016b, 35: 593-604.

Ghanbari, E., Abbasi, M.A., Dehghanpour, H., et al. Flowback volumetric and chemical analysis for evaluating load recovery and its impact on early-time production. Paper SPE 167165 Presented at the SPE Unconventional Resources Conference Canada, Calgary, Alberta, Canada, 5-7 November, 2013.

Guo, C.H., Xu, J.C., Wu, K.L., et al. Study on gas flow through nano pores of shale gas reservoirs. Fuel 2015, 143: 107-117.

Haber, J. Manual on catalyst characterization. Pure Appl. Chem. 1991, 63(9): 1227-1246.

Hill, R.J., Jarvie, D.M., Zumberge, J., et al. Oil and gas geochemistry and petroleum systems of the Fort Worth basin. AAPG Bull. 2007, 91(4): 445-473.

Javadpour, F. Nanopores and apparent permeability of gas flow in mudrocks (shales and siltstone). J. Can. Pet. Technol. 2009, 48(8): 16-21.

Javadpour, F., Fisher, D., Unsworth, M. Nanoscale gas flow in shale gas sediments. J. Can. Pet. Technol. 2007, 46(10): 55-61.

Javadpour, F., McClure, M., Naraghi, M.E. Slip-corrected liquid permeability and its effect on hydraulic fracturing and fluid loss in shale. Fuel 2015, 160: 549-559.

Javadpour, F., Moravvej Farshi, M., Amrein, M. Atomic-force microscopy: A new tool for gas-shale characterization. J. Can. Pet. Technol. 2012, 51(4): 236-243.

Katsube, T. Shale permeability and pore-structure evolution characteristics. Nat. Resour. Can. 2000, 1: 1-9.

King, G.E. Hydraulic fracturing 101: What every representative, environmentalist, regulator, reporter, investor, university researcher, neighbor and engineer should know about estimating frac risk and improving frac performance in unconventional gas and oil wells. Paper SPE 152596 Presented at the SPE Hydraulic Fracturing Technology Conference, The Woodlands, Texas, USA, 6-8 February, 2012.

King Jr, H.E., Eberle, A.P., Walters, C.C., et al. Pore architecture and connectivity in gas shale. Energy Fuels 2015, 29(3): 1375-1390.

Klinkenberg, L. The permeability of porous media to liquids and gases. Paper API41200 Presented at the Drilling and Production Practice, New York, USA, 1 January, 1941.

Langmuir, I. The adsorption of gases on plane surface of glass, mica and platinum. J. Am. Chem. Soc. 1918, 40(9): 1361-1403.

Liu, D., Ge, H., Liu, J., et al. Experimental investigation on aqueous phase migration in unconventional gas reservoir rock samples by nuclear magnetic resonance. J. Nat. Gas Sci. Eng. 2016a, 36: 837-851.

Liu, X.J., Xiong, J., Liang, L.X. Investigation of pore structure and fractal characteristics of organic-rich Yanchang formation shale in central China by nitrogen adsorption/desorption analysis. J. Nat. Gas Sci. Eng. 2015, 22: 62-72.

Loucks, R.G., Reed, R.M., Ruppel, S.C., et al. Spectrum of pore types and networks in mudrocks and a descriptive classification for matrix-related mudrock pores. AAPG Bull. 2012, 96(6): 1071-1098.

Makhanov, K., Dehghanpour, H., Kuru, E. An experimental study of spontaneous imbibition in Horn River shales. Paper SPE 162650 Presented at the SPE Canadian Unconventional Resources Conference, Calgary, Alberta, Canada, 30 October-1 November, 2012.

Meng, M., Ge, H., Ji, W., et al. Monitor the process of shale spontaneous imbibition in co-current and counter-current displacing gas by using low field nuclear magnetic resonance method. J. Nat. Gas Sci. Eng. 2015a, 27: 336-345.

Meng, M., Ge, H., Ji, W., et al. Investigation on the variation of shale permeability with spontaneous imbibition time: Sandstones and volcanic rocks as comparative study. J. Nat. Gas Sci. Eng. 2015b, 27: 1546-1554.

Meng, M., Ge, H., Ji, W., et al. Research on the auto-removal mechanism of shale aqueous phase trapping using low field nuclear magnetic resonance technique. J. Pet. Sci. Eng. 2016, 137: 63-73.

Milliken, K.L., Rudnicki, M., Awwiller, D.N., et al. Organic matter-hosted pore system, Marcellus Formation (Devonian), Pennsylvania. AAPG Bull. 2013, 97(2): 177-200.

Moghanloo, R.G., Yuan, B., Ingrahama, N., et al. Applying macroscopic material balance to evaluate interplay between dynamic drainage volume and well performance in tight formations. J. Nat. Gas Sci. Eng. 2015, 27: 466-478.

Odumabo, S.M., Karpyn, Z.T. Investigation of gas flow hindrance due to fracturing fluid leakoff in low permeability sandstones. J. Nat. Gas Sci. Eng. 2014, 17: 1-12.

Palisch, T.T., Vincent, M., Handren, P.J. Slickwater fracturing: Food for thought. SPE Prod. Oper. 2010, 25(3): 327-344.

Penny, G.S., Dobkins, T.A., Pursley, J.T. Field study of completion fluids to enhance gas production in the Barnett shale. SPE Gas Technology Symposium, 2006.

Qin, Y., Wang, Y., Yang, X., et al. Experimental study on dynamic gas adsorption. Int. J. Min. Sci. Technol. 2012, 22(6): 763-767.

Ren, W.X., Li, G.S., Tian, S.C., et al. An analytical model for real gas flow in shale nanopores with non-circular cross-section. AlChE J. 2016, 62(8): 2893-2901.

Rezaee, R. Fundamentals of gas shale reservoirs. New Jersey, USA, John Wiley & Sons, 2015.

Roy, S., Raju, R., Chuang, H.F., et al. Modeling gas flow through microchannels and nanopores. J. Appl. Phys. 2003, 93(8): 4870-4879.

Roychaudhuri, B., Tsotsis, T.T., Jessen, K. An experimental investigation of spontaneous imbibition in gas shales. J. Pet. Sci. Eng. 2013, 111: 87-97.

Shen, Y., Ge, H., Li, C., et al. Water imbibition of shale and its potential influence on shale gas recovery-a comparative study of marine and continental shale formations. J. Nat. Gas Sci. Eng. 2016a, 35: 1121-1128.

Shen, Y., Ge, H., Su, S., et al. Imbibition characteristic of shale gas formation and water-block removal capability. Sci. Sin. Phys.. Mech. Astron. 2017, 47(11): 114609.

Shen, Y., Ge, H., Su, S., et al. Impact of capillary imbibition into shale on lost gas volume. Chem. Technol. Fuels Oils 2016b, 52(5): 536-541.

Sheng, M., Li, G., Tian, S., et al. A fractal permeability model for shale matrix with multi-scale porous structure. Fractals 2016, 24(1): 1650002.

Sheng, M., Li, G.S., Huang, Z.W., et al. Pore-scale modeling and analysis of surface diffusion effects on shale-gas flow

in kerogen pores. J. Nat. Gas Sci. Eng. 2015, 27: 979-985.

Soliman, M., Daal, J., East, L. Fracturing unconventional formations to enhance productivity. J. Nat. Gas Sci. Eng. 2012, 8: 52-67.

Sondergeld, C.H., Ambrose, R.J., Rai, C.S., et al. Microstructural studies of gas shales. Paper SPE 131771 Presented at the SPE Unconventional Gas Conference, Pittsburgh, Pennsylvania, USA, 23-25 February, 2010.

Song, B., Economides, M.J., Ehlig-Economides, C.A. Design of multiple transverse fracture horizontal wells in shale gas reservoirs. Paper SPE 140555 Presented at the SPE Hydraulic Fracturing Technology Conference, The Woodlands, Texas, USA, 24-26 January, 2011.

Strapoc, D., Mastalerz, M., Schimmelmann, A., et al. Geochemical constraints on the origin and volume of gas in the New Albany Shale (Devonian-Mississippian), eastern Illinois Basin. AAPG Bull. 2010, 94(11): 1713-1740.

Thompson, S.L., Owens, W.R. A survey of flow at low pressures. Vacuum 1975, 25(4): 151-156.

Wang, D., Butler, R., Liu, H., et al. Flow-rate behavior and imbibition in shale. SPE Reserv. Eval. Eng. 2011, 14(4): 485-492.

Wang, J., Dong, M., Yang, Z., et al. Investigation of methane desorption and its effect on the gas production process from shale: Experimental and mathematical study. Energy Fuels 2017, 31(1): 216.

Wang, J., Yang, Z., Dong, M., et al. Experimental and numerical investigation of dynamic gas adsorption/desorption-diffusion process in shale. Energy Fuels 2016a, 30(12): 10080-10091.

Wang, J.J., Wang, B.E., Li, Y.J., et al. Measurement of dynamic adsorption-diffusion process of methane in shale. Fuel 2016b, 172: 37-48.

Wang, R., Zhang, K., Detpunyawat, P., et al. Analytical solution of matrix permeability of organic-rich shale. Paper IPTC18627 Presented at the International Petroleum Technology Conference, Bangkok, Thailand, 14-16 November, 2016d.

Wang, Z.Y., Jin, X., Wang, X.Q., et al. Pore-scale geometry effects on gas permeability in shale. J. Nat. Gas Sci. Eng. 2016d, 34: 948-957.

Wu, K., Chen, Z., Li, X. Real gas transport through nanopores of varying cross-section type and shape in shale gas reservoirs. Chem. Eng. J. 2015a, 281: 813-825.

Wu, K., Li, X., Guo, C., et al. Adsorbed gas surface diffusion and bulk gas transport in nanopores of shale reservoirs with real gas effect-adsorption-mechanical coupling. Paper SPE 173201 Presented at the SPE Reservoir Simulation Symposium, Houston, Texas, USA, 23-25 February, 2015b.

Wu, K., Li, X., Wang, C., et al. Apparent permeability for gas flow in shale reservoirs coupling effects of gas diffusion and desorption. Paper URTeC1921039 Presented at the Unconventional Resources Technology Conference, Denver, Colorado, USA, 25-27 August, 2014.

Wu, K., Li, X., Wang, C., et al. Model for surface diffusion of adsorbed gas in nanopores of shale gas reservoirs. Ind. Eng. Chem. Res. 2015c, 54(12): 3225-3236.

Wu, K.L., Chen, Z.X., Li, X.F., et al. A model for multiple transport mechanisms through nanopores of shale gas reservoirs with real gas effect-adsorption-mechanic coupling. Int. J. Heat Mass Transf. 2016, 93: 408-426.

Yaich, E., Williams, S., Bowser, A., et al. A case study: The impact of soaking on well performance in the Marcellus. Paper URTeC2154766 Presented at the Unconventional Resources Technology Conference San Antonio, Texas, USA, 20-22 July, 2015.

Yang, F., Ning, Z.F., Liu, H.Q. Fractal characteristics of shales from a shale gas reservoir in the Sichuan Basin, China. Fuel 2014, 115: 378-384.

Yang, L., Ge, H., Shi, X., et al. The effect of microstructure and rock mineralogy on water imbibition characteristics in tight reservoirs. J. Nat. Gas Sci. Eng. 2016a, 34: 1461-1471.

Yang, L., Ge, H., Shi, X., et al. Experimental and numerical study on the relationship between water imbibition and salt ion diffusion in fractured shale reservoirs. J. Nat. Gas Sci. Eng. 2017, 38: 283-297.

Yang, Z.H., Wang, W.H., Dong, M.Z., et al. A model of dynamic adsorption-diffusion for modeling gas transport and storage in shale. Fuel 2016b, 173: 115-128.

Yao, J., Sun, H., Fan, D.Y., et al. Numerical simulation of gas transport mechanisms in tight shale gas reservoirs. Pet. Sci. 2013, 10(4): 528-537.

Yuan, B., Moghanloo, R.G., Wang, K., et al. An integrated approach for fracturing evaluation and optimization using rate-transient analysis and dynamic drainage volume. Paper SPE 182244 Presented at the SPE Asia Pacific Oil & Gas Conference and Exhibition, Perth, Australia, 25-27 October, 2016a.

Yuan, Y.D., Doonechaly, N.G., Rahman, S. An analytical model of apparent gas permeability for tight porous media. Transp. Porous Media 2016b, 111(1): 193-214.

Zhang, T., Ellis, G.S., Ruppel, S.C., et al. Effect of organic-matter type and thermal maturity on methane adsorption in shale-gas systems. Org. Geochem. 2012, 47: 120-131.

Zheng, Q., Yu, B., Duan, Y., et al. A fractal model for gas slippage factor in porous media in the slip flow regime. Chem. Eng. Sci. 2013, 87: 209-215.

Ziarani, A.S., Aguilera, R. Knudsen's permeability correction for tight porous media. Transp. Porous Media 2012, 91(1): 239-260.